Characterization of the *Neospora caninum* NcROP40 and NcROP2Fam-1 rhoptry proteins during the tachyzoite lytic cycle

IVÁN PASTOR-FERNÁNDEZ[1], JAVIER REGIDOR-CERRILLO[1], ELENA JIMÉNEZ-RUIZ[1], GEMA ÁLVAREZ-GARCÍA[1], VIRGINIA MARUGÁN-HERNÁNDEZ[1], ANDREW HEMPHILL[2] *and* LUIS M. ORTEGA-MORA[1]*

[1] *SALUVET, Animal Health Department, Faculty of Veterinary Sciences, Complutense University of Madrid, Ciudad Universitaria s/n, 28040-Madrid, Spain*
[2] *Institute of Parasitology, Vetsuisse Faculty, University of Berne, Länggass-Strasse 122, CH-3012 Berne, Switzerland*

(*Received 27 July 2015; revised 5 October 2015; accepted 10 October 2015; first published online 2 November 2015*)

SUMMARY

Virulence factors from the ROP2-family have been extensively studied in *Toxoplasma gondii*, but in the closely related *Neospora caninum* only NcROP2Fam-1 has been partially characterized to date. NcROP40 is a member of this family and was found to be more abundantly expressed in virulent isolates. Both NcROP2Fam-1 and NcROP40 were evaluated as vaccine candidates and exerted a synergistic effect in terms of protection against vertical transmission in mouse models, which suggests that they may be relevant for parasite pathogenicity. NcROP40 is localized in the rhoptry bulbs of tachyzoites and bradyzoites, but in contrast to NcROP2Fam-1, the protein does not associate with the parasitophorous vacuole membrane due to the lack of arginine-rich amphipathic helix in its sequence. Similarly to Nc*ROP2Fam-1*, Nc*ROP40* mRNA levels are highly increased during tachyzoite egress and invasion. However, Nc*ROP40* up-regulation does not appear to be linked to the mechanisms triggering egress. In contrast to NcROP2Fam-1, phosphorylation of NcROP40 was not observed during egress. Besides, NcROP40 secretion into the host cell was not successfully detected by immunofluorescence techniques. These findings indicate that NcROP40 and NcROP2Fam-1 carry out different functions, and highlight the need to elucidate the role of NcROP40 within the lytic cycle and to explain its relative abundance in tachyzoites.

Key words: *Neospora caninum*, NcROP40, NcROP2Fam-1, characterization, *in silico* analysis, lytic cycle of tachyzoites, immunolocalization, secretion assays, mRNA expression profile, protein phosphorylation.

INTRODUCTION

Neospora caninum is a cyst-forming parasite that causes neuromuscular disorders in dogs, and abortion, stillbirth and birth of weak offspring in bovines. This protozoan is phylogenetically related to *Toxoplasma gondii*, with which it shares the ability to cross the placenta and to infect the foetus. In cattle, asexually proliferating tachyzoites and bradyzoites are the only stages described. Tachyzoites have a high proliferative potential and are thus responsible for the dissemination of the parasite into different tissues. Bradyzoites ensure parasite persistence by forming tissue cysts located in immune-privileged organs such as the brain (Dubey and Schares, 2011). Since these two stages are strictly intracellular, they have developed a number of mechanisms to actively invade their host cells and modulate their intracellular compartment to optimize intracellular survival and growth. These processes are grouped under the name of lytic cycle (Hemphill *et al*. 2013). Important structures exclusively found in apicomplexans, namely the apical complex and specialized secretory organelles such as micronemes, rhoptries and dense granules play important roles in the lytic cycle. Contents of these secretory organelles are sequentially released to ensure invasion, intracellular maintenance and replication of the parasite in parasitophorous vacuoles, where they mediate and influence the host-cell machinery (Kemp *et al*. 2013). Among apicomplexan parasites, the molecular basis of the lytic cycle is highly conserved, and the underlying of mechanisms described for *T. gondii* (Carruthers and Sibley, 1997) and *Plasmodium* spp. (Cowman *et al*. 2012) are likely to be similar in *N. caninum* (Hemphill *et al*. 2013).

Rhoptries have been the subject of extensive studies during the last years due to the role of their proteins in host-cell invasion and cell regulation processes. Some of these proteins (RONs) are restricted to the neck, and others (ROPs) to the bulb of these organelles. RONs are involved in the formation of the moving junction required for parasite entry into the host cells (Beck *et al*. 2014). The ROP2-family represents one of the largest and best-studied

* Corresponding author: SALUVET, Animal Health Department, Faculty of Veterinary Sciences, Complutense University of Madrid, Ciudad Universitaria s/n, 28040-Madrid, Spain. E-mail: luis.ortega@vet.ucm.es

doi:10.1017/S0031182015001511

group of ROP proteins in *T. gondii*, and includes protein kinases and pseudokinases that are proven virulence factors (Schneider *et al*. 2013; Etheridge *et al*. 2014; Lei *et al*. 2014; Reese *et al*. 2014). To our knowledge, most of the ROP2-like proteins are secreted into the host cytosol during invasion and some of them can associate with the parasitophorous vacuole membrane (PVM), but their function is still largely unknown (El Hajj *et al*. 2006; Bradley and Sibley, 2007; Boothroyd and Dubremetz, 2008). The ROP2-family has been recently catalogued in *N. caninum* (Talevich and Kannan, 2013), but only limited information is available on this protein family. Currently, only NcROP1, NcROP2Fam-1, NcROP4, NcROP5, NcROP9, NcROP30 and NcROP40 have been identified by proteomic studies (Marugán-Hernández *et al*. 2011; Sohn *et al*. 2011; Regidor-Cerrillo *et al*. 2012), but their function has not been described. To date, the only *N. caninum* rhoptry protein that has been partially characterized is NcROP2Fam-1 (Alaeddine *et al*. 2013). This protein was previously considered the orthologue of TgROP7 (Reid *et al*. 2012). However, it has been recently shown that TgROP7 and NcROP2Fam-1 are unlikely to be orthologues (Alaeddine *et al*. 2013). A fragment of NcROP2Fam-1 has been employed as a vaccine in mouse models, showing relatively high protection rates against challenge infection (Debache *et al*. 2008, 2009, 2010). Another rhoptry protein, NcROP40, was found to be more abundantly expressed in virulent isolates of *N. caninum* (Regidor-Cerrillo *et al*. 2012), thus posing the obvious question whether NcROP40 plays a potential role in parasite virulence as described for other rhoptry proteins in *T. gondii*. When applied as vaccines a combined NcROP40 + NcROP2Fam-1 protein formulation had a synergistic effect and was able to induce a partial block in transplacental transmission in a pregnant mouse model of neosporosis (Pastor-Fernández *et al*. 2015).

The aim of the present work was to characterize NcROP40 and compare its features with NcROP2Fam-1 during the lytic cycle of *N. caninum* development. This includes the molecular characterization of the NcROP40 through *in silico* studies, define its subcellular localization throughout the lytic cycle in comparison with NcROP2Fam-1, and to study protein dynamics, the transcript expression profile and their phosphorylation in order to predict their putative functional role in the different phases of the tachyzoite lytic cycle.

MATERIALS AND METHODS

*In silico analysis and Nc*ROP40 *sequencing*

All the sequences were obtained from ToxoDB v7.3. and v12 (www.toxodb.org) and edited using the BioEdit software v7·1.1. BLAST tools from NCBI (www.ncbi.nlm.nih.gov/BLAST/) and ToxoDB websites were used to match homologous sequences. Clustal Omega (http://www.ebi.ac.uk/Tools/msa/clustalo/) was employed to align nucleotide and protein sequences. Identity and similarity percentages were calculated with the Sequence Manipulation Suite (http://www.bioinformatics.org/sms2/ident_sim.html). Open Reading Frames (ORFs) and introns were predicted through the ORF Finder Tool (www.ncbi.nlm.nih.gov/gorf/gorf.html), NCBI and the Splign Tool (www.ncbi.nlm.nih.gov/sutils/splign/splign.cgi), respectively. SignalP 4·1server (www.cbs.dtu.dk/services/SignalP/) CBS was used to predict signal peptide. Potential alpha helices in the arginine-rich amphipathic helix (RAH) domain were searched using Jpred3 (http://www.compbio.dundee.ac.uk/www-jpred/), PSIPRED v3.0 (http://bioinf.cs.ucl.ac.uk/psipred/) and PSSpred (http://zhanglab.ccmb.med.umich.edu/PSSpred/) tools. Trans-membrane regions were predicted with the TMPred tool (www.ch.embnet.org/software/TMPRED_form.html, ExPASy) and protein families from Pfam database (http://pfam.sanger.ac.uk Sanger). Potential phosphorylation sites were analysed by the NetPhos v2.0 (http://www.cbs.dtu.dk/services/NetPhos/), NetPhosK v1.0 (http://www.cbs.dtu.dk/services/NetPhosK/) and the Diphos v1.3 (http://www.dabi.temple.edu/disphos/) servers.

The Nc*ROP40* gene (previously named Nc*ROP8*, NCLIV_012920 in ToxoDB v12) was sequenced and compared among three *N. caninum* isolates of different origins. For this purpose, total genomic DNA from Nc-Liv (Barber *et al*. 1993), Nc-Spain7 (Regidor-Cerrillo *et al*. 2008) and Nc-Spain1H (Rojo-Montejo *et al*. 2009) isolates was purified with the DNeasy Blood & Tissue Kit (Qiagen) following the manufacturer's recommendations. The *NcROP40*-ORF (1176 bp) and the up and down-stream regions (750 + 992 bp) were amplified from the three isolates using the Fw-chrV_ROP40 and Rv-chrV_ROP40 primers (Additional file 1). PCR conditions were 95 °C for 5 min, 35 cycles at 95 °C for 1 min, 58 °C for 1 min and 72 °C for 1 min, and a final elongation at 72 °C for 10 min. PCRs were carried out with the Platinum® Taq DNA Polymerase High Fidelity (Invitrogen) and all primers were purchased from Sigma-Aldrich. Amplified fragments were purified with the GENECLEAN Turbo kit (MP Biomedicals) from 1% low-melting agarose gels. DNA was sequenced in two directions with an ABI Prism 377 DNA sequencer (Applied Biosystems) in the Genomics Unit of the Scientific Park of Madrid. Six pairs of primers were employed for this purpose (Additional file 1). Sequences were edited and aligned using the BioEdit software v7.1.1.

Parasite culture

Neospora caninum (Nc-Liv isolate) tachyzoites were propagated *in vitro* by continuous passage in MARC-145 cell culture using standard procedures (Pérez-Zaballos *et al*. 2005). For transmission electron microscopy, murine epidermal keratinocyte cultures were infected with the same isolate as described earlier (Vonlaufen *et al*. 2002). *In vitro* tachyzoite-to-bradyzoite stage conversion was induced and checked by BAG1 and CC2 expression as previously described (Hemphill *et al*. 2004). Evacuole assays were performed with the Nc-Liv isolate in human foreskin fibroblasts (HFFs) as previously described (Dunn *et al*. 2008).

Generation of plasmids

Nc*ROP40* (NCLIV_012920 in ToxoDB v12) and Nc*ROP2Fam-1* (NCLIV_001970 in ToxoDB v12) were cloned in the pET45b(+) expression system (Novagen) as previously described (Pastor-Fernández *et al*. 2015; Regidor-Cerrillo *et al*. 2012). On the other hand, Nc*Alpha-Tubulin* (*TUBα*) (NCLIV_058890 in ToxoDB v12) and Nc*SAG1* (NCLIV_033230 in ToxoDB v12) fragments were amplified from *N. caninum* cDNA and cloned within the pGEM-T-Easy vector (Promega). Primer sequences for cloning are summarized in Additional file 2. All primers were purchased from Sigma-Aldrich, and the Expand High Fidelity Plus PCR System (Roche) was used for all PCRs. Amplicons were purified with the GENECLEAN Turbo kit (MP Biomedicals) from 1% low-melting agarose gels (Lonza).

Production of recombinant proteins, mass spectrometry (MS) analysis and sodium dodecyl sulphate-polyacrylamide gel electrophoresis (SDS–PAGE)

Escherichia coli NovaBlue Single Competent Cells (Novagen) were transformed with construct-containing plasmids, which were isolated using the QIAprep Spin Miniprep Kit (Qiagen) and sequenced with an ABI Prism 377 DNA sequencer (Applied Biosystems) using T7 forward and reverse primers in the Genomics Unit of the Scientific Park of Madrid. All sequences were aligned with 100% consensus.

Escherichia coli BL21(DE3) pLysS competent cells (Agilent Technologies) were transformed with the resulting expression vectors and foreign expression of rNcROP40 and rNcROP2Fam-1 as a (His) 6-tagged fusion proteins was carried out following standard procedures (Álvarez-García *et al*. 2007). Denatured proteins were on-column refolded and purified using HisTrapHP columns coupled to the ÄKTAprime Plus system (GE Healthcare) as previously described (Pastor-Fernández *et al*. 2015). Recombinant proteins included the whole Nc*ROP40* sequence [1–392 amino acids (aa)] and the C-terminus domains for rNcROP2Fam-1 (238–594 aa), excluding the RAH domains. Concentration and purity of recombinant proteins was checked by SDS–PAGE with a standard bovine serum albumin (BSA) scale (Roche) and using the GS-800 densitometer coupled to the Quantity One software (Bio-Rad Laboratories) (Álvarez-García *et al*. 2007). Electrophoresed proteins were manually excised from prepared Coomassie-stained one-dimensional (1D) gels for MS analysis (peptide mass fingerprinting) following standard procedures (Risco-Castillo *et al*. 2007).

Polyclonal antibody (PAb) production and affinity purification

Polyclonal sera against rNcROP40 (Regidor-Cerrillo *et al*. 2012) and rNcROP2Fam-1 were raised in New Zealand White rabbits (Harlan Laboratories) following a procedure previously described (Risco-Castillo *et al*. 2007). Samples of pre-immune serum were collected to confirm the absence of antibodies against *N. caninum* by Western Blot. All protocols followed the proceedings detailed by the current legislation at the time of the experiment (Spanish Royal Decree 1201/2005) and were approved by the Animal Research Committee of the Complutense University. Affinity purified antibodies were prepared from PAbs following standard procedures (Álvarez-García *et al*. 2007).

Immunoblots

Detection of NcROP40 and NcROP2Fam-1 proteins in parasite extracts was carried out by Western Blot following SDS–PAGE under reducing conditions. Unless otherwise stated, all reagents were purchased from Bio-Rad Laboratories. 2×10^7 purified Nc-Liv tachyzoites were disrupted by bath-sonication, electrophoresed in 15% bis-acrylamide gels and transferred onto nitrocellulose membranes according to standard procedures. PAbs *α*-rNcROP40 and *α*-rNcROP2Fam-1 were diluted at 1:5000. Goat anti-rabbit IgG antibody conjugated to peroxidase (Sigma-Aldrich) was used as secondary antibody at 1:25 000 dilution. Reactions were developed by chemiluminiscence with the Immobilon Western Chemiluminescent HRP substrate (Millipore). For image acquisition, AGFA films (Curix/RP2 Plus) and AGFA CP1000 processor were used after 1–30 s of exposure time.

Immunogold-labelling and transmission electron microscopy (TEM)

Infected keratinocyte cultures were fixed and LR-White embedded and on-section labelled as

previously described (Risco-Castillo *et al*. 2007). Affinity-purified rabbit α-rNcROP40 was diluted 1:2 in PBS–0·3% BSA and sections were incubated for 1 h in a moist chamber. They were then washed in three changes of PBS, 10 min each, and goat anti-rabbit conjugated to 10 nm diameter gold particles (Amersham) was applied at a dilution of 1:5 in PBS–0·3% BSA as secondary antibody. After another three washes, 10 min each, grids were air dried and contrasted with uranyle acetate and lead citrate (Hemphill *et al*. 2004). Specimens were viewed on a Phillips 600 TEM operating at 60 kV.

Immunofluorescence staining

Protein localization dynamics in *N. caninum* tachyzoites were studied on infected MARC-145 cells on rounded coverslips at different time-points after infection. A total of 5×10^4 cells were placed on sterile 13 mm-coverslips onto 24-well plates and incubated overnight at 37 °C on a 5% CO_2 atmosphere. Then, tachyzoites were scrapped from culture flasks, passed through a 21-gauge needle and counted on a haemacytometer by trypan blue exclusion. Subsequently, MARC-145 monolayers were infected with *N. caninum* for 20 and 40 min (MOI 3), 1, 2, 6 (MOI 3), 24, 32 (MOI 2) and 48 h (MOI 1). After infection, non-adherent parasites were removed from coverslips by three PBS washes. Then, three methods of fixation were employed. Absolute methanol, 2% paraformaldehyde in PBS and 2% paraformaldehyde–0·05% glutaraldehyde in PBS were used as fixatives for 10–30 min at room temperature. All samples were immediately processed for immunofluorescence staining.

Coverslips were blocked and permeabilized with PBS containing 3% BSA (Roche) and 0·25% Triton X-100 (Merck Chemicals) for 30 min at 37 °C. Then, cultures were labelled with the monoclonal antibody (MAb) α-NcSAG1 as a surface marker [(Björkman and Hemphill, 1998); 1:250 dilution] and affinity purified PAbs α-NcROP40 and α-NcROP2Fam-1 (1:8 dilution) by incubation for 1 h at room temperature. Following three washes with PBS, coverslips were incubated with Alexa Fluor 488-conjugated goat anti-mouse IgG and Alexa Fluor 594-conjugated goat anti-rabbit IgG at 1:1000 dilution (Molecular Probes) for 1 h at room temperature. Nuclei were stained with 4′,6-diamidino-2-phenylindole dye (DAPI, Lonza) at 1:5000 dilution in PBS. Finally, coverslips were mounted on glass slides with ProLong® Gold antifade reagent (Molecular Probes). Evacuoles were detected on infected HFFs in the presence of cythochalasin D following the same protocol (Additional file 5).

To phalloidin staining, coverslips fixed in 2% paraformaldehyde were blocked, permeabilized and labelled with MAb α-NcSAG1 and affinity purified PAb α-NcROP2Fam-1 as described above. After washing, they were incubated with Alexa Fluor 647-conjugated goat anti-mouse IgG (1:1000), Alexa Fluor 488-conjugated goat anti-rabbit IgG (1:1000), phalloidin–TRITC (1:250) (Sigma-Aldrich) and DAPI dyed.

Single 1 μm slices of immunofluorescence stainings were captured with a Leica TCS–SPE confocal laser-scanning microscope (Leica Microsystems) in the Department of Biochemistry and Molecular Biology IV of the Complutense University (Madrid). Image processing was performed using the LAS AF (Leica Microsystems) and the ImageJ software (NCBI, http://rsb.info.nih.gov/ij/).

Secretion assays

Secretion assays were performed with tachyzoites obtained from cultures prior to egress. For this purpose, parasites were scrapped from culture flasks, pelleted by centrifugation (1350 × ***g***, 10 min, 4 °C), passed through a 21-gauge needle and purified by PD-10 desalting columns (GE Healthcare). Then, 1×10^8 tachyzoites were placed on 500 μL of cold phenol red-free DMEM (Life-Technologies) and stimulated with either 10 μM calcium ionophore A23187 (Sigma-Aldrich), 1% ethanol (Merck Chemicals) or 10 mM dithiothreitol (DTT, Calbiochem) for 20 min at 37 °C (Naguleswaran *et al*. 2001). Non-stimulated parasites were kept on ice during the same period of time. After the incubation, secretion supernatants were recovered by double centrifugation (1350 × ***g***, 10 min, 4 °C and 8000 × ***g***, 10 min, 4 °C), passed through 0·2 μm polyvinylidene difluoride (PVDF) filters (Whatman, GE Healthcare) and supplemented with phosphatase and protease inhibitor cocktails (Sigma-Aldrich). Pelleted parasites were washed once in cold PBS supplemented with phosphatase and protease inhibitor cocktails, and recovered by centrifugation (1350 × ***g***, 10 min, 4 °C). All samples were stored at −80 °C until further analyses.

Supernatants and pellets were analysed by immunoblotting, and secretion was estimated by comparing equal amounts of secretion supernatants and tachyzoite lysates. Monoclonal antibodies directed against NcTUBα (α-TUBα MAb, Sigma-Aldrich) were used on immunoblots of secreted supernatant fractions to monitor tachyzoite lysis, and antibodies directed against NcMIC2 were used as a positive control of secretion (Lovett *et al*. 2000). The α-TUBα MAb specifically recognized NcTUBα protein in tachyzoite extracts. PVDF membranes were incubated with rabbit α-rNcROP40, α-rNcROP2Fam-1 and α-rNcMIC2 at 1:5000 dilutions, whereas α-TUBα MAb was employed at 1:10 000 dilution. Secondary antibodies were employed at 1:25 000 (goat anti-rabbit IgG antibody conjugated to peroxidase) and at 1:80 000 dilutions (goat anti-mouse IgG antibody conjugated to peroxidase)

(Sigma-Aldrich). Reactions were developed by chemiluminiscence with the Immobilon Western Chemiluminescent HRP Substrate as describe above.

*Evaluation of Nc*ROP40 *and Nc*ROP2Fam-1 *mRNA expression levels*

The mRNA expression levels of Nc*ROP40* and Nc*ROP2Fam-1* were assessed by real-time reverse transcription PCR throughout the lytic cycle of tachyzoites at four representative points which illustrate the recent invasion, PV formation and maturation, exponential growth of parasites and tachyzoite egress. For this purpose, MARC-145 cultures were infected with the Nc-Liv isolate at MOI 3 for 6, 24, 48 and 56 h. Infected cultures were synchronized by washing the monolayer twice with pre-warmed PBS and replacing the culture media at 6 h post infection (hpi), to remove non-adherent parasites. Cells were harvested with a cell scraper and recovered by centrifugation at 1350 × ***g*** for 15 min at 4 °C. Pelleted parasites were conserved at −80 °C until RNA extraction. The experiment was carried out in triplicate. For each experiment, three different flasks were analysed at each time-point. The effect of induced egress of tachyzoites on expression levels of Nc*ROP40* and Nc*ROP2Fam-1* was also studied in parallel. For this purpose, five flasks from three different experiments containing cells that were infected for 48 h were treated with 10 mM DTT for 1 h, after which tachyzoites had undergone egress from approximately 80% of parasitophorous vacuoles. Tachyzoites were then recovered as described above.

Total RNA was extracted using the Maxwell® 16 LEV simplyRNA Purification Kit (Promega) that includes a DNAse treatment, following the manufacturer's recommendations. RNA concentrations were determined by spectrophotometry (Nanophotometer, Implen), and RNA integrity was checked by the visualization of the 18S and 28S ribosomal fragments after electrophoresis on 1% agarose gels. Reverse transcription was carried out by the master mix SuperScript® VILO™ cDNA Synthesis Kit (Invitrogen) in a 20 μL reaction using 2·5 μg of total RNA. Resulting cDNA was diluted 1:20 and analysed by real-time PCR.

Real-time PCR reactions were performed using the Power SYBR® Green PCR Master Mix in the ABI 7300 Real Time PCR System (Applied Biosystems) following standard conditions. Primers used for amplification of Nc*ROP40*, Nc*ROP2Fam-1* and the housekeeping genes Nc*TUBα* and Nc*SAG1* are shown in Table 1. A seven-point duplicate standard curve based on 10-fold serial dilutions was included on each run. pET45b(+)-Nc*ROP40*, pET45b(+)-Nc*ROP2Fam-1*, pGEM-T-Nc*TUBα* and pGEM-T-Nc*SAG1* plasmids were used as standards.

mRNA expression levels for each target were normalized by the −ΔCt method (Schmittgen and

Table 1. Primers used to amplify Nc*ROP40*, Nc*ROP2Fam-1*, Nc*SAG1* and Nc*Tubilin alpha* sequences by real-time-PCR

Protein	ToxoDB accession number	Primer sequences	Reference	Length	Introns[a]	Slope[b]	R^{2b}
Nc*ROP40*	NCLIV_012920	Fw-CATCAAGCAGCCCCAGAATCA Rv-TGGTGACTGCGACCAACTTA	This study	94 bp. 1021–1114	No	−3·71	0·996
Nc*ROP2Fam-1*	NCLIV_001970	Fw-TTCTTCCTCTCCAAGCGACA Rv-TTGAGTCGTTCCCGAAGTTG	Alaeddine *et al.* (2013)	140 bp. 1604–1743	No	−3·68	0·996
Nc*SAG1*	NCLIV_033230	Fw-CGGTGTCGCAATGTGCTCTT Rv-ACGGTCGTCCCAGAACAAAC	Fernández-García *et al.* (2006)	150 bp. 504–653	No	−3·24	0·997
Nc*TUBα*	NCLIV_058890	Fw-GGTAACGCCTGCTGGGAG Rv-GCTCCAAATCCAAGAAGACGCA	Alaeddine *et al.* (2013)	166 bp. 49–214	Yes*	−3·24	0·994

* Forward primer for Nc*TUBα* amplification annealed at intron splice junction to prevent amplification of genomic DNA.
[a] Primers for intron-containing sequences were designed using cDNA as template.
[b] Descriptive values of real time-PCR from standard curves for each pair of primers are shown.

Livak, 2008). −ΔCt values were calculated by subtracting the Ct value of the normalizer genes from the Ct value of each sample. Relative fold increases or decreases were assessed by the $2^{-\Delta\Delta Ct}$ method (Schmittgen and Livak, 2008). Since expression levels at 24 hpi were the lowest for both proteins, the −ΔΔCt value was calculated by subtracting the mean −ΔCt values for each protein at 24 hpi as baseline samples as indicated in this formula: −ΔΔCt = −[(Ct Nc*ROPx*–Ct Nc*TUBα*)–(mean Ct Nc*ROPx* at 24 h–mean Ct Nc*TUBα* at 24 h)]. Raw RNA samples were included in each batch of amplifications to confirm the absence of *N. caninum* genomic DNA. Data analyses of mRNA expression levels were carried out by Kruskal–Wallis and Dunn's tests using GraphPad Prism v6.01 software.

Phosphorylation assays

Phosphorylation assays were performed on denatured lysates generated from infected MARC-145 cell cultures at 56 hpi, when tachyzoite had escaped from parasitophorous vacuoles and invaded neighbouring cells. Freshly pelleted cell monolayers were resuspended on alkaline phosphatase-compatible buffer [100 mM sodium chloride (Panreac), 50 mM Tris–HCl (Panreac), 10 mM magnesium chloride (Merck Chemicals), 1 mM DTT (Calbiochem), 0·2% Triton X-100 (Merck Chemicals) and protease inhibitor cocktail (Sigma-Aldrich) (pH 7·9) or in phosphatase inhibitor buffer (50 mM) HEPES (Sigma-Aldrich), 100 mM sodium fluoride (Sigma-Aldrich), 2 mM sodium orthovanadate (Sigma-Aldrich), 2 mM EDTA (Sigma-Aldrich), 1 mM DTT, 0·2% Triton X-100 and protease inhibitor cocktail]. Extracts were disrupted on ice for 15 min by bath-sonication (Ultrasons, Selecta), and shaked by vortexing during an additional 45 min. Alkaline phosphatase treatment (20 U CIP/2×10^7 tachyzoites, New England Biolabs) was only applied on extracts resuspended in alkaline phosphatase-compatible buffer for 90 min at 37 °C. Resulting extracts were stored at −80 °C until further analysis.

Phosphorylated proteins experience a mobility shift on Phos-tag SDS–PAGE electrophoresis (Kinoshita *et al*. 2006). To determine if NcROP40 and NcROP2Fam-1 are phosphorylated, tachyzoite extracts resuspended in alkaline phosphatase-compatible buffer (CIP) and phosphatase inhibitor buffer (PI) were electrophoresed in 15% bis-acrylamide gels supplemented with 25 μM Phos-Tag (Wako Pure Chemicals Industries) and 50 μM manganese (II) chloride (Merck Chemicals). After electrophoresis, gels were washed once in 0·1 M EDTA in transfer buffer and once in transfer buffer without EDTA to remove metal complexes. Then, gels were transferred onto nitrocellulose membranes according to standard procedures. Membranes were incubated with α-rNcROP40 and α-rNcROP2Fam-1 at 1:1000 dilution, and then incubated with goat anti-rabbit IgG antibody conjugated to peroxidase at 1:1000 dilution. Reactions were developed using 4-chloro-1-naphtol as substrate until signal visualization.

RESULTS

*In silico analysis and Nc*ROP40 *sequencing*

Nc*ROP40* (NCLIV_012920, chromosome V) is currently classified as an unspecified product, but in previous releases of ToxoDB (v7·3) the protein was named as rhoptry kinase family protein ROP40 and considered as orthologous gene of Tg*ROP40*. No introns are predicted in the Nc*ROP40* sequence, which contains 1176 bp and codes for a product of a predicted molecular weight of 43 kDa. In contrast, the Tg*ROP40* sequence (TGME49_291960, chromosome IX) contains two introns, a coding sequence of 1578 bp and a predicted molecular weight of 57·9 kDa. However, according to previous releases of ToxoDB (v7·3), the Tg*ROP40* gene (TGME49_091960) has no introns. The predicted peptide sequences of NcROP40 and TgROP40 proteins (v7·3) share 32·3% identity and 48·7% similarity. In addition, a Pfam database search identified a protein kinase-like domain in NcROP40, but catalytic activity is lacking (PANDIT: PF14531).

Due to the observed inconsistencies between Nc*ROP40* and Tg*ROP40*, the chromosome V-sequence of the *N. caninum* Nc-Liv genome was analysed in detail. First, the N-terminus of the Nc*ROP40* sequence was strikingly shorter than that annotated for Tg*ROP40* (~400 bp). In order to elucidate these differences, up and down-stream Nc*ROP40* sequences (from positions 662772 to 665947, chromosome V) were submitted to the ORF Finder tool, which displayed a unique 1578 bp ORF, which corresponds to a putative protein with a calculated molecular weight of 57·8 kDa. This finding is consistent with the Tg*ROP40* sequence. The presence of the additional N-terminal fragment in the Nc*ROP40* ORF was confirmed by RT–PCR using cDNA from tachyzoites at two different time points of infection (Additional file 3). The newly identified ORF (now termed Nc*ROP40-long*) contains the Nc*ROP40* sequence as listed in ToxoDB and an additional 402 bp at its N-terminus (Additional file 4) (GenBank: KP731805, KP731806 and KP731807). According to the previous Tg*ROP40* gene (TGME49_091960 in ToxoDB v7·3), no introns were predicted when the Nc*ROP40-long* DNA sequence was submitted to the Splign tool. The percentage of aa sequence identity between TgROP40 and NcROP40-long increased from 32·3 to 42·9, whilst similarity increased from 46·3 to 61·4% (Fig. 1A).

Protein trans-membrane regions were predicted for the NcROP40-long protein between the positions

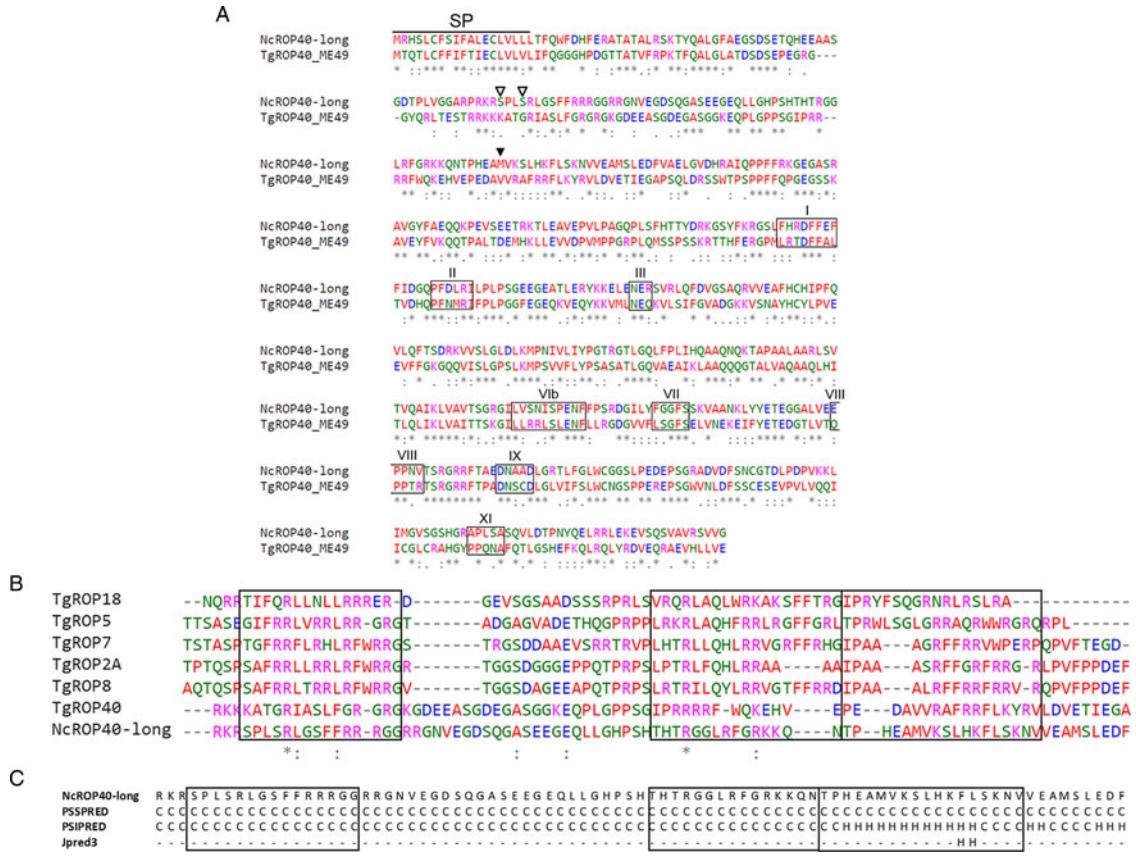

Fig. 1. (A) Sequence alignment of the ROP40 protein, both in *N. caninum* (NCLIV_012920) and *T. gondii* (TGME49_091960). NcROP40-long is referred to the NcROP40 sequence incorporating and additional 134 aa in the N-terminus. SP: signal peptide. Empty arrow head: potential phosphorylation sites. Filled arrow head: origin of the NcROP40 protein as shown in ToxoDB. Boxes and roman numerals: conserved motifs of likely inactive rhoptry kinase regions as described for Talevich and colleagues in 2013. (B) Comparison of the RAH domains among rhoptry proteins from the ROP2-family. Boxes designate the three domains described for El Hajj and colleagues in 2006. Sequences were obtained from ToxoDB with the following accession numbers: TGME49_005250 (TgROP18), TGME49_108080 (TgROP5), TGME49_095110 (TgROP7), TGME49_015780 (TgROP2A), TGME49_015770 (TgROP8), TGME49_091960 (TgROP40) and NCLIV_012920 (NcROP40). For A and B asterisks (*) indicate fully conserved residues, whilst colons (:) and periods (·) indicate conservation between groups of strongly or weakly similar properties, respectively. (C) Secondary structure predictions of the NcROP40-long RAH domains by PSSpred, PSIPRED and Jpred3 servers. (H) helix. (C) coil. Dashes: undefined.

5 and 25, but according to SignalP predictions the signal peptide is cleaved between aa 19 and 20. Sequence comparison among the most representative members of the ROP2-family (Fig. 1B), as well as alpha helices prediction within the structure of the NcROP40-long protein (Fig. 1C), suggest that the protein lacks RAH domains. Phosphorylation sites both in NcROP40-long and NcROP2Fam-1 were subjected to three different prediction programs (NetPhos v2.0, NetPhosK v1.0 and Diphos v1.3.), and were only considered when detected by at least two of them. In this sense, NcROP40 showed two putative phosphorylation sites at position S-75 and S-78, whilst phosphorylation of NcROP2Fam-1 was predicted to occur at positions S-82 and S-129.

The Nc*ROP40-long* ORF and its up and downstream sequences were amplified by PCR from DNA of three different isolates, which have shown manifest differences in virulence: Nc-Liv, Nc-Spain7 and Nc-Spain1H. Primers were designed to amplify a fragment of 2918 bp, containing the ORF. After PCR, amplicons were sequenced and analysed in detail. For all isolates a 2362 bp consensus fragment was sequenced in two directions. This fragment comprised the Nc*ROP40-long* ORF (1578 bp) and an additional 148 and 636 bp in its flanking regions. Thus, comparative analyses did not show differences in the amplified sequences among the three isolates (Additional file 4).

Protein sequence and immunodetection

The identities of rNcROP40 and rNcROP2Fam-1 were confirmed by mass spectrometric analyses. rNcROP40 matched with the NCLIV_012920 sequence (score: 175; 18/60 matched values; 64% of sequence coverage), whereas rNcROP2Fam-1 matched with the NCLIV_001970 annotation

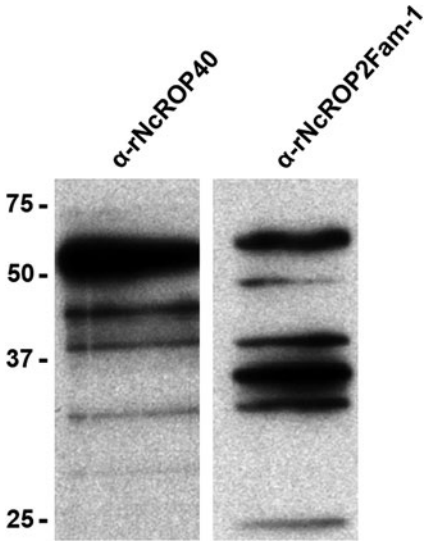

Fig. 2. *Neospora caninum*-based Western-blot showing the immuno-reactivity of α-rNcROP40 and α-rNcROP2Fam-1 antibodies. Five bands of approximately 53, 44, 38, 32 and 28 kDa were detected with α-NcROP40 antibodies, whilst six different bands of approximately 58, 48, 40, 36, 34 and 26 kDa were detected with α-NcROP2Fam-1 antibodies.

(score: 345; 33/65 matched values; 69% of sequence coverage). These analyses corroborated the composition of both proteins, with a molecular weight of 43·9 and 43·2 kDa, respectively, according to the predicted molecular weights of rNcROP40 and rNcROP2Fam-1, which exclude part of their N-terminal domains. Hence, rNcROP40 and rNcROP2Fam-1 were used to develop PAbs in rabbits. *Neospora caninum* tachyzoite crude extracts were separated by SDS–PAGE under reducing conditions. Western blots revealed that α-NcROP40 reacted with five distinct bands of approximately 53, 44, 38, 32 and 28 kDa. The polyclonal α-NcROP2Fam-1 antiserum detected six different bands of approximately 58, 48, 40, 36, 34 and 26 kDa (Fig. 2).

Subcellular localization of NcROP40 by TEM

In order to confirm the subcellular localization of NcROP40, immunogold-TEM was carried out on sections of keratinocytes infected with *N. caninum* tachyzoites, and of cultures infected with bradyzoites generated *in vitro* by sodium nitroprusside treatment. In both, *N. caninum* tachyzoites (Fig. 3A and B) and *in vitro* induced-bradyzoites (Fig. 3C and D), affinity-purified anti-NcROP40 antibodies localized to rhoptry bulbs.

NcROP40 and NcROP2Fam-1 tracing throughout the lytic cycle

Immunofluorescence staining of NcROP40 on *N. caninum*-infected cultures showed a rhoptry-like pattern in tachyzoites throughout the lytic cycle, from 20 min to 56 hpi. Methanol fixation showed the clearest results in terms of NcROP40 immunolocalization. In contrast, fixation with paraformaldehyde and glutaraldehyde mixtures resulted in a lower staining intensity (Fig. 4). The rhoptry-like pattern was clearly associated with the apical end of tachyzoites in all the micrographs, and disappeared as the captured slices intersected the parasites in more external areas (Fig. 4, 24 and 32 hpi, MeOH fixation). Interestingly, the presence of NcROP40 was not detected, neither in evacuoles during the invasion phases nor in the PVM during the development and establishment of the PV, with similar results obtained using three different fixation protocols. Hence, no secretion of NcROP40 protein could be detected under the tested conditions.

Concerning NcROP2Fam-1, our PAbs specifically recognized rhoptry-like structures at the parasite apex at all time-points as described for NcROP40. In contrast, secretion of the protein was detected from 20 min to 24 hpi using all three fixation protocols (Fig. 5). Specifically, evacuoles were detected from 20 min to 6 hpi. These rhoptry-derived secretory vesicles were localized intracellularly and surrounded the host-cell nucleus, as shown by the phalloidin stainings in those coverslips fixed with paraformaldehyde (Fig. 5, 6 h, PFA fixation). At later time points, during the establishment of the PV, NcROP2Fam-1 was detected on the PVM (Fig. 5, 6 hpi) and in the PV matrix (Fig. 5, 24 hpi) under all the fixation methods. Thereafter, NcROP2Fam-1 was restricted to rhoptries (Fig. 5, 32 and 48 hpi). Interestingly, the protein was released again during egress, where it appeared to localize on the surface of the extracellular tachyzoites (Fig. 5, 56 hpi).

Identical results were obtained for NcROP40 and NcROP2Fam-1 proteins by specific evacuole assays carried out in HFFs (Additional file 5).

Induced secretion of NcROP40 and NcROP2Fam-1

Freshly purified tachyzoites were treated with A23187, ethanol or DTT in order to induce the calcium-related protein secretion from apical organelles. However, NcROP40 and NcROP2Fam-1 proteins were not detected on secretome supernatants by immunoblotting. In contrast, a manifest secretion of the NcMIC2 protein was observed under the same conditions, according to previous findings (Lovett *et al*. 2000). Moreover, inadvertent lysis of tachyzoites during these secretion assays could be discarded since no NcTUBα could be detected in any of the secreted fractions (Additional file 6).

*Nc*ROP40 *and Nc*ROP2Fam-1 *mRNA expression during the lytic cycle*

Nc*ROP40* and Nc*ROP2Fam-1* transcription levels were monitored at four representative time points

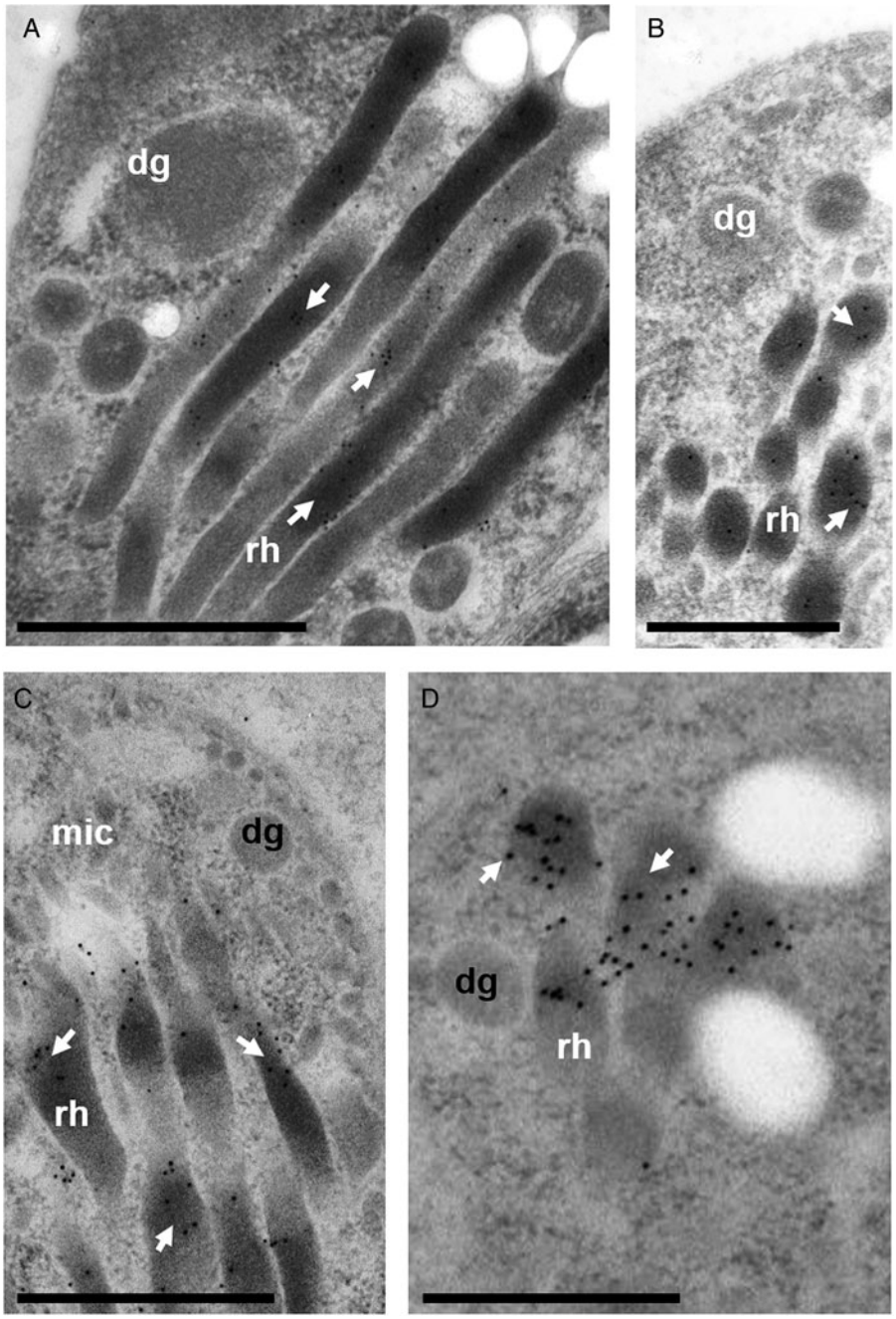

Fig. 3. NcROP40 is a rhoptry protein associated with rhoptry bulbs. TEM and immunogold staining in tachyzoites (A,B) and bradyzoites (C,D). Rhoptries (rh), dense granules (dg) and micronemes (mic) are indicated on the pictures. Bars represent 1 μm.

during the lytic cycle. Similar results in the mRNA pattern were observed using Nc*TUBα* and Nc*SAG1* as normalizer genes (data not shown). The results presented here were processed using Nc*TUBα* as normalizer.

The lowest Nc*ROP40* and Nc*ROP2Fam-1* mRNA levels were found at 24 hpi. In contrast, mRNA levels were the highest at 6 hpi (during the invasion phase) and at 56 hpi (egress phase) for both proteins ($P < 0{\cdot}005$; Kruskal–Wallis test) (Fig. 6A). Differences in fold increases of mRNA transcription were calculated by the $2^{-\Delta\Delta Ct}$ method. Since the lowest normalized values for both Nc*ROP40* and Nc*ROP2Fam-1* were observed at 24 hpi, this time point was used as baseline to calculate the mRNA transcription fold increases during egress and invasion. Nc*ROP40* showed a 4-fold increase in mRNA levels at 6 and 56 hpi, and Nc*ROP2Fam-1* exhibited a 3-fold increase at the same time points. At 48 hpi, mRNA levels displayed a 2-fold increase for both Nc*ROP40* and Nc*ROP2Fam-1*.

Egress of *N. caninum* and *T. gondii* tachyzoites can be artificially induced *in vitro* by the addition of DTT into the culture medium. Thus, the effect of DTT supplementation on the expression of Nc*ROP40*

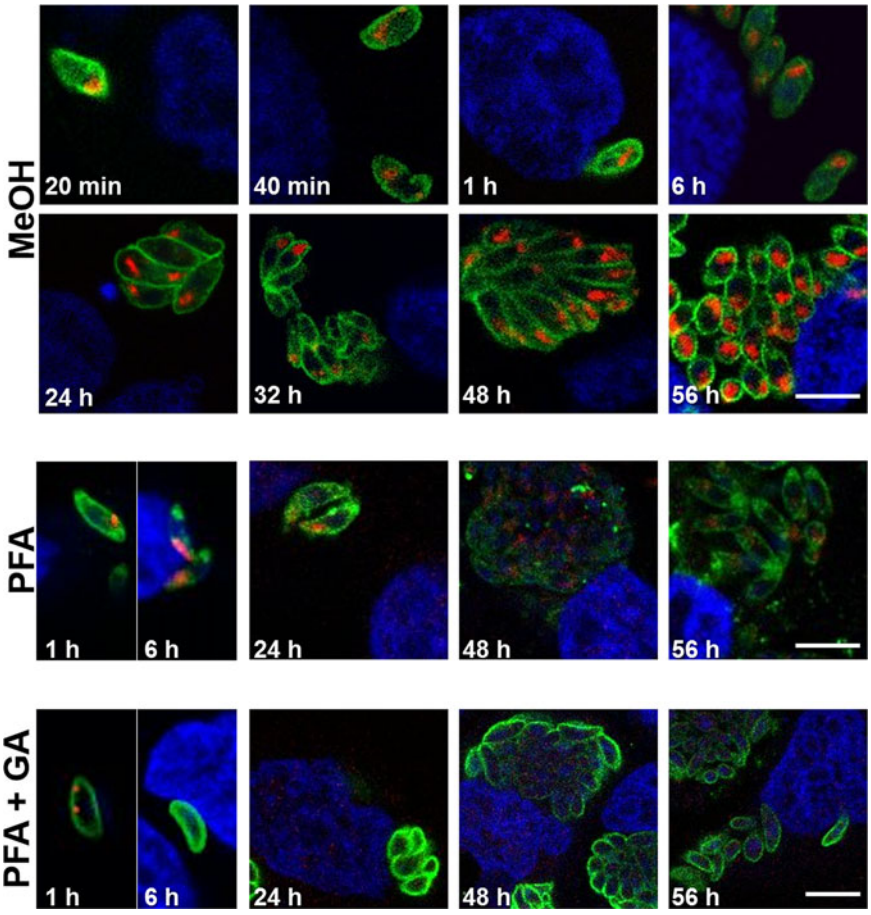

Fig. 4. Confocal laser scanning microscopy of NcROP40 along the lytic cycle of tachyzoites. Infected cultures were fixed with metanol (MeOH), paraformaldehyde (PFA) and paraformaldehyde combined with glutaraldehyde (PFA + GA) and double labelled with affinity purified antibodies against NcROP40 (red) and monoclonal antibodies against NcSAG1 (green). Nuclei were stained with DAPI (blue). All the images show a single 1 μm slice. Bars represent 4 μm.

and Nc*ROP2Fam-1* mRNA was studied. Different responses were observed: while Nc*ROP40* did not exhibit significant increases in its mRNA levels upon DTT treatment, Nc*ROP2Fam-1* mRNA transcription was significantly increased ($P < 0{\cdot}005$; Kruskal–Wallis test) (Fig. 6B). Moreover, mean values for Nc*ROP2Fam-1* mRNA remained above those observed at 56 hpi, while the corresponding values for Nc*ROP40* remained below (Fig. 6B).

Phosphorylation of NcROP40 and NcROP2Fam-1 at the egress

The phosphorylation status of NcROP40 and NcROP2Fam-1 was studied at 56 hpi, as this was the time point when the mRNA levels for both proteins within the lytic cycle were the highest, simultaneously to tachyzoite egress and early invasion. Tachyzoites were harvested, processed under conditions that preserve the phosphorylation status, and extracts were separated by Phos-Tag SDS–PAGE electrophoresis. The electrophoretic mobility of NcROP40 on Phos-Tag gels was similar in both, alkaline phosphatase-treated and phosphatase inhibitor-treated extracts. In contrast, NcROP2Fam-1 showed a mobility shift in those extracts treated with phosphatase inhibitors, which suggests that NcROP2Fam-1 is phosphorylated at 56 hpi (Fig. 7).

DISCUSSION

Considerable efforts have been undertaken to increase the understanding on how apicomplexan parasites interact with their host cells and how they maintain and optimize their intracellular life style. It is widely known that components of distinct secretory organelles, namely rhoptries, micronemes and dense granules, play a crucial role in defining the host–parasite relationship (Carruthers and Sibley, 1997) and therefore corresponding antigens are being extensively studied as vaccine targets to prevent infections by apicomplexan parasites.

TgROP proteins have shown to be important virulence factors (Lim *et al*. 2012). In contrast, little is known about the rhoptry proteins in *N. caninum*. Several NcROP and NcRON proteins have been identified by different proteomic approaches and monoclonal antibodies (Straub *et al*. 2009; Marugán-Hernández *et al*. 2011; Sohn *et al*. 2011; Regidor-Cerrillo *et al*. 2012), but only

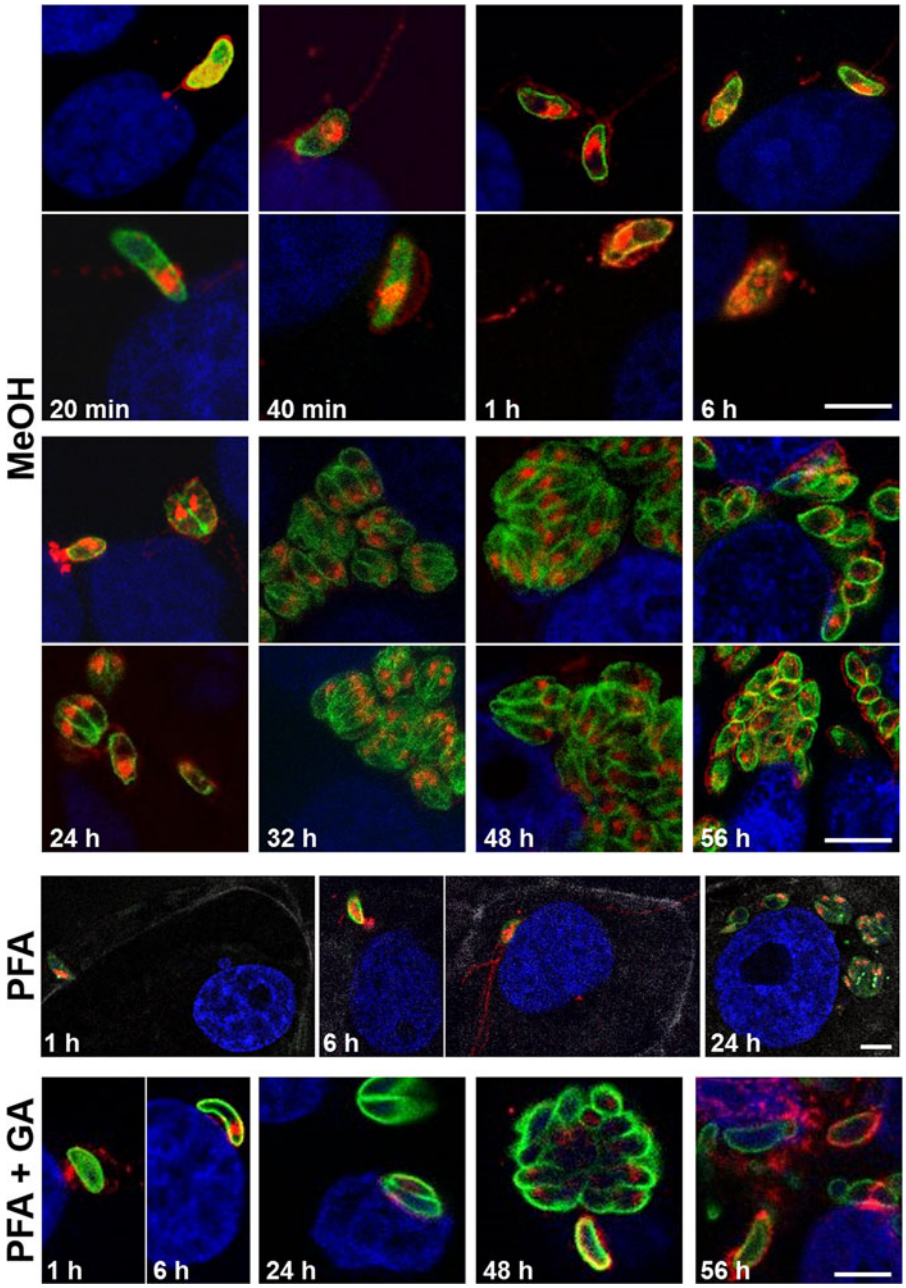

Fig. 5. Confocal laser scanning microscopy of NcROP2Fam-1 along the lytic cycle of tachyzoites. Infected cultures were fixed with metanol (MeOH), paraformaldehyde (PFA) and paraformaldehyde combined with glutaraldehyde (PFA + GA) and double labelled with affinity purified antibodies against NcROP2Fam-1 (red) and monoclonal antibodies against NcSAG1 (green). Nuclei were stained with DAPI (blue). PFA-fixed cultures were also labelled with phalloidin to delimitate host-cell surface (white). All the images show a single 1 μm slice. Bars represent 4 μm.

NcROP2Fam-1, which has been associated with the tachyzoites invasion process, has been partially characterized to date (Alaeddine *et al*. 2013).

NcROP40 was shown to be more abundant in virulent isolates of *N. caninum* (Regidor-Cerrillo *et al*. 2012). In *T. gondii*, limited information is available for the orthologous gene product Tg*ROP40* (initially named as TgROP2L6). Tg*ROP40* is highly expressed in tachyzoites (Peixoto *et al*. 2010) and increased expression levels were observed during acute infections in mice (Pittman *et al*. 2014). A number of studies suggested that NcROP40 is one of the major rhoptry components, since it has been detected by three different proteomic approaches (Marugán-Hernández *et al*. 2011; Regidor-Cerrillo *et al*. 2012; Pollo-Oliveira *et al*. 2013). Hence, NcROP40 expression could be an important element related to parasite virulence. Indeed, a vaccine formulation combining NcROP40 + NcROP2Fam-1 recombinant proteins was recently assessed in a pregnant mouse model of neosporosis and conferred partial protection against congenital transmission of *N. caninum*, with NcROP40 and NcROP2Fam-1 acting synergistically (Pastor-Fernández *et al*. 2015).

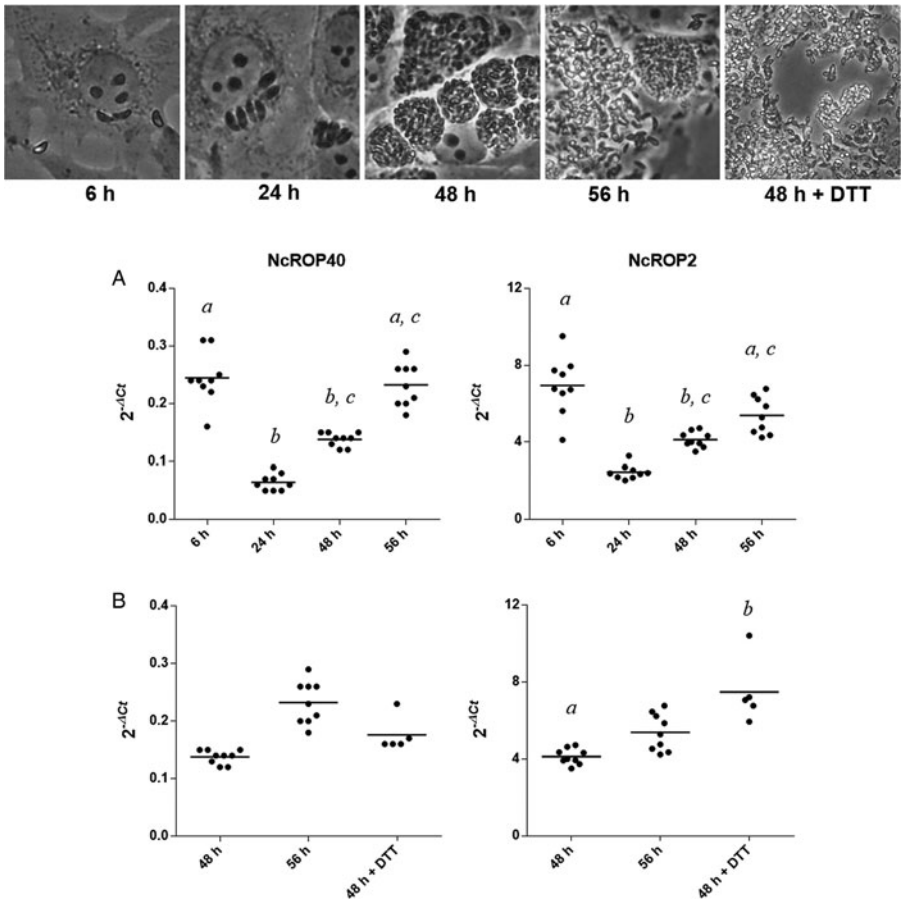

Fig. 6. mRNA expression of Nc*ROP40* and Nc*ROP2Fam-1*. Real time-PCR was employed to assess the mRNA expression of both proteins along the lytic cycle. Top panel: photomicrographs showing the infection dynamics of the Nc-Liv isolate on MARC-145 cultures at recent invasion (6 h), PV formation and maturation (24 h), exponential growth of parasites (48 h) and tachyzoite egress (56 and 48 h + DTT). (A) mRNA expression levels of Nc*ROP40* and Nc*ROP2Fam-1* during the lytic cycle. (B) Effect of DTT supplementation to artificially induce egress at 48 h on mRNA expression for both proteins. For (A) and (B), each point represents a single sample and bars represent the mean value. *a*, *b* and *c* indicate significant differences ($P < 0{\cdot}005$; Kruskal–Wallis test).

Comparison of the Nc*ROP40* ORF and its potential regulatory expression sequences among three different *N. caninum* isolates with differing virulence and *in vitro* behaviour (Pereira García-Melo *et al*. 2010; Regidor-Cerrillo *et al*. 2010; Regidor-Cerrillo *et al*. 2011) did not reveal any polymorphism that could explain differences in virulence as described for TgROP18 (Steinfeldt *et al*. 2010). However, dissimilarities in protein abundance among isolates might be due to regulatory mechanisms such as epigenetics, which have been shown to be involved in genome reprogramming during tachyzoite to bradyzoite conversion in *T. gondii* (Dixon *et al*. 2010). These analyses allowed a detailed dissection of the Nc*ROP40* gene, including flanking regions, and lead to the description of the Nc*ROP40-long* sequence (Nc*ROP40* sequence with an additional 402 bp in its N-terminus), whose presence was confirmed by RT–PCR (Additional file 3). In addition, an improved transcriptome annotation for *NcROP40* has recently been submitted (GenBank: CEL65449·1), confirming our results (Ramaprasad *et al*. 2015).

Inconsistencies in the measured (53 kDa) and theoretical (58 kDa) molecular weight of NcROP40-long, as well as the presence of different bands on immunoblots, could reflect the maturation process described for all ROP2-family rhoptry proteins, which are synthesized as pro-proteins (Hajagos *et al*. 2012). In fact, Alaeddine and colleagues described the processing of the NcROP2Fam-1 protein by Western Blot through different affinity purified antibodies directed against peptides located at the C-terminal end of the protein (Alaeddine *et al*. 2013). In *T. gondii* TgSUB2 protease is in charge to remove the N-terminal domains that are involved in rhoptry targeting at a highly conserved SΦ*x*(E/D) site (Hajagos *et al*. 2012). This sequence was also found in the N-terminal domain of NcROP2Fam-1 (Alaeddine *et al*. 2013), but is absent in NcROP40. In any case, the PAb recognizes a main band of 53 kDa and a number of additional bands by Western blotting, which may reflect a protein maturation process. Nevertheless, further studies must be carried out to define more accurately the implication of these changes on protein function.

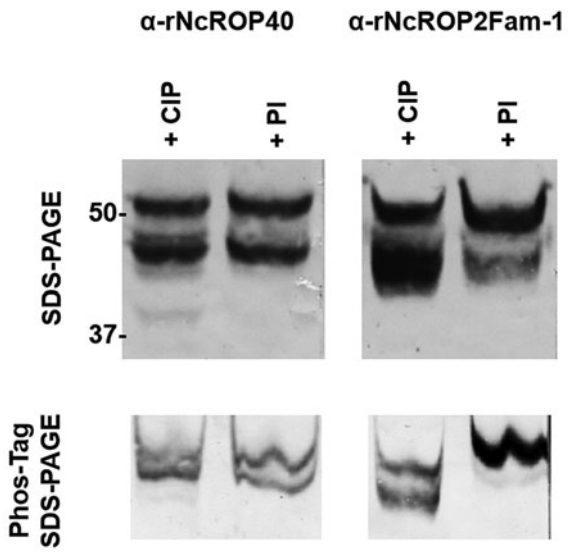

Fig. 7. Phosphorylation detection of NcROP40 and NcROP2Fam-1 by Phos-Tag SDS–PAGE. Tachyzoite extracts obtained at 56 hpi were processed with alkaline phosphatase (CIP) and phosphatase inhibitors (PI), electrophoresed on SDS–PAGE and Phos-Tag SDS–PAGE gels, and blotted to nitrocellulose membranes. Then, both proteins were detected by their respective antibodies in order to detect a mobility shift of the proteins treated with PI.

In silico analyses are useful to predict certain protein features, and were employed in this study to further characterize the NcROP40 protein. The presence of a signal peptide is an important prerequisite for a protein to enter the secretory pathway in eukaryotes, and putative signal peptides are present in both TgROP40 (El Hajj *et al*. 2006) and NcROP40 (this work). This is in contrast with our observations, since NcROP40 secretion is not detected by immunofluorescence microscopy, even when employing three different fixation protocols or specific evacuole assays. Moreover, NcROP40 does not interact with the PVM, albeit this finding is consistent with the predicted lack of RAH domains in its sequence. RAH domains are the regions displaying the highest similarities between each of the members of the ROP2-family, and are required for PVM association. These domains are also absent in the TgROP40 protein, and consequently it does not associate with the PVM (El Hajj *et al*. 2006; Reese and Boothroyd, 2009). Nevertheless, previous studies carried out with the toxofilin protein of *T. gondii* showed that secretion of low abundance proteins may be undetectable by immunofluorescence approaches, which is especially relevant for those proteins that are not concentrated on a membrane or in an intracellular compartment (Lodoen *et al*. 2009). This may be the case for the NcROP40 protein that could be secreted into the host-cell cytosol. Interestingly, the TgROP40 protein shows some nuclear localization when is heterologously expressed in infected HFF, suggesting that the protein may be translocated into the host-cell nucleus after its secretion in the cytosol. Nevertheless, the immunodetection of the NcROP40 into the host-cell nucleus was not achieved in this study (Reese and Boothroyd, 2009). In contrast to NcROP40, NcROP2Fam-1 was extensively secreted under the tested conditions (Alaeddine *et al*. 2013). The protein was easily detected in evacuoles, and then surrounding invasive tachyzoites from 1 to 24 hpi. Similar findings have been described for the TgROP2 protein, which may participate in the PVM formation (Beckers *et al*. 1994; Sinai and Joiner, 2001; Nakaar *et al*. 2003; Dunn *et al*. 2008). Consistent with our findings, most of the rhoptry proteins described to date in *T. gondii* are secreted and participate in host-cell invasion, PV formation and maturation, and/or are involved in hijacking the host-cell machinery (Kemp *et al*. 2013).

On the other hand, we could not detect any NcROP40 and NcROP2Fam-1 protein in the secretory fractions after induction of tachyzoite secretion using A23187, ethanol or DTT stimulation. This indicates that rhoptry discharge is not affected by elevated intracellular calcium levels as previously stated for *T. gondii* rhoptry proteins (Carruthers and Sibley, 1999), and that rhoptry secretion can be only induced upon host-cell contact.

The mRNA levels of Nc*ROP40* and Nc*ROP2Fam-1* transcripts were quantified during defined time points of the lytic cycle of tachyzoites grown in MARC-145 cells (Regidor-Cerrillo *et al*. 2011). Both proteins displayed higher mRNA levels at 6 hpi (which largely represents recently invaded tachyzoites) and at 56 hpi (representing tachyzoites shortly prior to or already undergoing egress). Lower mRNA levels were measured at 24 hpi (a time point representing early exponential replication). Subsequently, once exponential growth of parasites was almost completed (48 hpi), mRNA levels of Nc*ROP40* and Nc*ROP2Fam-1* gradually increased to reach again their highest value. According to our findings, developmental transitions in *Plasmodium falciparum* and *T. gondii* have shown to be strongly influenced by changes in mRNA levels (Le Roch *et al*. 2004; Radke *et al*. 2005). Indeed, a modal switch from expression of proteins involved in invasion and motility has been also described in extracellular tachyzoites of *T. gondii* (Lescault *et al*. 2010; Gaji *et al*. 2011). This could suggest that Nc*ROP40* and Nc*ROP2Fam-1* proteins are required for the subsequent phases of the lytic cycle in which both are highly transcribed. This phenomenon is consistent with the 'just-in-time' concept stated for *P. falciparum* and *T. gondii*, whereby gene expression is only activated as their biological function becomes necessary to the parasite (Llinas and DeRisi, 2004; Radke *et al*. 2005; Behnke *et al*. 2010).

In addition to monitoring mRNA levels during egress under normal culture conditions, the same was done by inducing egress artificially employing DTT at 48 hpi (Esposito *et al*. 2007). DTT treatment induced a dramatic increase in Nc*ROP2Fam-1* expression after DTT supplementation, to levels similar to naturally occurring egress. Strikingly, and in contrast to Nc*ROP2Fam-1*, Nc*ROP40* mRNA levels were not substantially increased by DTT addition. To date, the mechanisms governing egress are not fully understood, but mounting evidence shows that intracellular calcium levels trigger the abrupt exit of parasites from PV, which is accompanied with a rapid decrease in host-cell ATP (Blackman and Carruthers, 2013). Nc*ROP40* mRNA levels were unresponsive to the artificially induced egress, suggesting that its upregulation does not rely on the mechanisms triggering egress in contrast to Nc*ROP2Fam-1*.

Phosphorylation has a prominent key role in cellular regulatory processes and influences the functional activity of a plethora of enzymes and structural proteins. At 56 hpi, when the mRNA expression levels for Nc*ROP40* and Nc*ROP2Fam-1* reached a peak and tachyzoites were undergoing egress to infect another host cell, phosphorylation was evident in NcROP2Fam-1, but not in NcROP40. However, we cannot exclude that NcROP40 is phosphorylated at another phase of the lytic cycle. Predicted phosphorylation sites were found in NcROP40 and in NcROP2Fam-1. However, it is important to note that the phosphorylation prediction algorithms are optimized for mammalian cells or other cell types, and that rhoptry proteins are unique among eukaryotes and are only found in apicomplexan parasites. Thus, potential phosphorylation sites might not be accurately predicted. Previous works have shown that TgROP2 and TgROP4 are also phosphorylated, but only in intracellular parasites, indicating that phosphorylation is associated with protein regulation and its potential participation within the lytic cycle (Carey *et al*. 2004; Dunn *et al*. 2008). For NcROP2Fam-1, phosphorylation coincides with high mRNA levels, and since NcROP2Fam-1 was shown to be involved in host-cell invasion (Alaeddine *et al*. 2013), this could indicate that the protein is being activated to prepare tachyzoites for egress and/or invasion. To date, there is no information about the relevance of phosphorylation in NcROP proteins, and phosphorylation of all the known TgROP proteins has not been studied. Previous works suggested that phosphorylation of dense granule proteins has an influence on PVM association (Labruyere *et al*. 1999; Mercier *et al*. 2005). Thus, phosphorylation of NcROP2Fam-1 could be important for secretion and its subsequent association to the PVM, and this could be also applied to TgROP2 and TgROP4, both of which exhibit similar properties. However, further studies must be carried out in order to determine the role of rhoptry protein phosphorylation during the lytic cycle of *N. caninum* tachyzoites.

Pseudokinases are emerging as key regulators of cellular signalling (Reese *et al*. 2014). Several studied rhoptry proteins in *T. gondii* have been described as kinases or pseudokinases, and some of them have shown the ability to remodel cellular transduction and the transcriptome of the host cell through phosphorylation events (Jacot and Soldati-Favre, 2012; Lim *et al*. 2012). Specifically, the TgROP18 and TgROP17 kinases and the TgROP5 pseudokinase form complexes and by that inactivate host immune responses and inflammation (Du *et al*. 2014; Etheridge *et al*. 2014). Moreover, TgROP16 regulates host innate immunity through STAT3 and STAT6 phosphorylation (Jensen *et al*. 2013) and TgROP38 modulates MAPK signalling to control apoptosis and cell proliferation (Peixoto *et al*. 2010). In our case, NcROP40 has been described as a predicted member of the rhoptry kinase family (ROPK) lacking the key kinase sequence motifs (Talevich and Kannan, 2013). The protein contains a structurally conserved N-terminal extension to the kinase domain that displays high sequence similarity to the NcROP5 and TgROP5 pseudokinases, among others. TgROP5 also lacks kinase activity (Reese and Boothroyd, 2011), but in contrast to NcROP40, is clearly secreted during invasion and associates with the PVM (El Hajj *et al*. 2007). Therefore, the role of NcROP40 as pseudokinase remains unclear. Nevertheless, the protein could be implicated in the regulation of still unknown virulence factors. Unfortunately, little is known about the existence of rhoptry virulence factors that could alter the host transcriptome after the infection with *N. caninum*. To date, the information about the orthologues of TgROP5, TgROP16, TgROP18 and TgROP38 in *N. caninum* is limited, and the only study in which they have been described is restricted to genomic and transcriptomic information that highlights the divergence of rhoptry proteins between *T. gondii* and *N. caninum* (Reid *et al*. 2012). Hence, despite the common features of *N. caninum* and *T. gondii*, these distinct differences in their secreted virulence factors make it difficult to make direct extrapolations from one species to the other. However, the description of common mechanisms of the ROP2-family members required for the success of the lytic cycle and parasite proliferation could represent a valuable source for the development of novel vaccine candidates.

In summary, this study describes highly interesting features of the NcROP40 protein, and another member of the ROP2-family, NcROP2Fam-1, during the lytic cycle of *N. caninum* tachyzoites. Immunogold TEM clearly localized NcROP40 in the rhoptry bulbs of *N. caninum* tachyzoites but, in contrast to NcROP2Fam-1, we were unable to

detect NcROP40 secretion into the host cell, which is likely an effect of the protein dilution within the host cytosol. mRNA quantification showed that Nc*ROP40* is highly expressed during egress and invasion, although its mRNA levels were not affected when egress was induced by DTT supplementation. These findings suggest differences in the transcriptional regulation and functional role of NcROP40 and NcROP2Fam-1. In addition, no evidence was found for NcROP40 phosphorylation at the time point of egress, in contrast to NcROP2Fam-1. NcROP40, together with NcROP2Fam-1, is a promising vaccine candidate, thus further studies will be carried out in order to elucidate its functionality. Epitope-tag assays and generation of Δ*rop40* knockout parasites would be useful to confirm more accurately whether NcROP40 is secreted or not, and to establish the role of the NcROP40 protein within the lytic cycle of *N. caninum*.

SUPPLEMENTARY MATERIAL

To view supplementary material for this article, please visit http://dx.doi.org/10.1017/S0031182015001511.

CONFLICT OF INTERESTS

The authors declare that they have no competing interests. The funders had no role in study design, data collection and analysis, decision to publish, or preparation of the manuscript.

AUTHOR CONTRIBUTIONS

JRC, GAG and LMOM conceived and designed the experiments. IPF, EJR, VMH and AH performed the experiments. IPF, JRC, GAG and LMOM analysed the data. IPF, JRC, EJR, GAG, VMH, AH and LMOM wrote the paper.

ACKNOWLEDGEMENTS

We gratefully acknowledge Professor Mª Teresa Miras Portugal's group from the Department of Biochemistry and Molecular Biology IV of the Complutense University (Madrid) for their confocal microscopy system. We also thank Dr Diana Williams from the Liverpool School of Tropical Medicine (Liverpool, UK) for the *N. caninum* Nc-Liv isolate and Dr David Sibley from the Washington University School of Medicine (St. Louis, MO, USA) for the NcMIC2 antibody.

FINANCIAL SUPPORT

This work was supported by the AGL2010-22191/GAN and the AGL2013-44694-R grants from the Spanish Ministry of Economy and Competitiveness (M.I.N.E.C.O.) and the S2013/ABI2906 grant from the Community of Madrid. Iván Pastor-Fernández was supported by a fellowship from the Spanish Ministry of Education, Culture and Sports (M.E.C.D.), as part of the Programme of Training of University Staff (F.P.U., grant no. AP2009-0354). Andrew Hemphill was supported by the Swiss National Science Foundation (grant no. 310030 146162).

REFERENCES

Alaeddine, F., Hemphill, A., Debache, K. and Guionaud, C. (2013). Molecular cloning and characterization of NcROP2Fam-1, a member of the ROP2 family of rhoptry proteins in *Neospora caninum* that is targeted by antibodies neutralizing host cell invasion *in vitro*. *Parasitology* **140**, 1033–1050.

Álvarez-García, G., Pitarch, A., Zaballos, A., Fernández-García, A., Gil, C., Gómez-Bautista, M., Aguado-Martínez, A. and Ortega-Mora, L. M. (2007). The NcGRA7 gene encodes the immunodominant 17 kDa antigen of *Neospora caninum*. *Parasitology* **134**, 41–50.

Barber, J., Trees, A. J., Owen, M. and Tennant, B. (1993). Isolation of *Neospora caninum* from a British dog. *The Veterinary Record* **133**, 531–532.

Beck, J. R., Chen, A. L., Kim, E. W. and Bradley, P. J. (2014). RON5 is critical for organization and function of the *Toxoplasma* moving junction complex. *PLoS Pathogens* **10**, e1004025.

Beckers, C. J., Dubremetz, J. F., Mercereau-Puijalon, O. and Joiner, K. A. (1994). The *Toxoplasma gondii* rhoptry protein ROP2 is inserted into the parasitophorous vacuole membrane, surrounding the intracellular parasite, and is exposed to the host cell cytoplasm. *The Journal of Cell Biology* **127**, 947–961.

Behnke, M. S., Wootton, J. C., Lehmann, M. M., Radke, J. B., Lucas, O., Nawas, J., Sibley, L. D. and White, M. W. (2010). Coordinated progression through two subtranscriptomes underlies the tachyzoite cycle of *Toxoplasma gondii*. *PLoS ONE* **5**, e12354.

Björkman, C. and Hemphill, A. (1998). Characterization of *Neospora caninum* iscom antigens using monoclonal antibodies. *Parasite Immunology* **20**, 73–80.

Blackman, M. J. and Carruthers, V. B. (2013). Recent insights into apicomplexan parasite egress provide new views to a kill. *Current Opinion in Microbiology* **16**, 459–464.

Boothroyd, J. C. and Dubremetz, J. F. (2008). Kiss and spit: the dual roles of *Toxoplasma* rhoptries. *Nature Reviews Microbiology* **6**, 79–88.

Bradley, P. J. and Sibley, L. D. (2007). Rhoptries: an arsenal of secreted virulence factors. *Current Opinion in Microbiology* **10**, 582–587.

Carey, K. L., Jongco, A. M., Kim, K. and Ward, G. E. (2004). The *Toxoplasma gondii* rhoptry protein ROP4 is secreted into the parasitophorous vacuole and becomes phosphorylated in infected cells. *Eukaryotic Cell* **3**, 1320–1330.

Carruthers, V. B. and Sibley, L. D. (1997). Sequential protein secretion from three distinct organelles of *Toxoplasma gondii* accompanies invasion of human fibroblasts. *European Journal of Cell Biology* **73**, 114–123.

Carruthers, V. B. and Sibley, L. D. (1999). Mobilization of intracellular calcium stimulates microneme discharge in *Toxoplasma gondii*. *Molecular Microbiology* **31**, 421–428.

Cowman, A. F., Berry, D. and Baum, J. (2012). The cellular and molecular basis for malaria parasite invasion of the human red blood cell. *The Journal of Cell Biology* **198**, 961–971.

Debache, K., Guionaud, C., Alaeddine, F., Mevissen, M. and Hemphill, A. (2008). Vaccination of mice with recombinant NcROP2 antigen reduces mortality and cerebral infection in mice infected with *Neospora caninum* tachyzoites. *International Journal for Parasitology* **38**, 1455–1463.

Debache, K., Alaeddine, F., Guionaud, C., Monney, T., Muller, J., Strohbusch, M., Leib, S. L., Grandgirard, D. and Hemphill, A. (2009). Vaccination with recombinant NcROP2 combined with recombinant NcMIC1 and NcMIC3 reduces cerebral infection and vertical transmission in mice experimentally infected with *Neospora caninum* tachyzoites. *International Journal for Parasitology* **39**, 1373–1384.

Debache, K., Guionaud, C., Alaeddine, F. and Hemphill, A. (2010). Intraperitoneal and intra-nasal vaccination of mice with three distinct recombinant *Neospora caninum* antigens results in differential effects with regard to protection against experimental challenge with *Neospora caninum* tachyzoites. *Parasitology* **137**, 229–240.

Dixon, S. E., Stilger, K. L., Elias, E. V., Naguleswaran, A. and Sullivan, W. J., Jr. (2010). A decade of epigenetic research in *Toxoplasma gondii*. *Molecular and Biochemical Parasitology* **173**, 1–9.

Du, J., An, R., Chen, L., Shen, Y., Chen, Y., Cheng, L., Jiang, Z., Zhang, A., Yu, L., Chu, D., Shen, Y., Luo, Q., Chen, H., Wan, L., Li, M., Xu, X. and Shen, J. (2014). *Toxoplasma gondii* virulence factor ROP18 inhibits the host NF-kappaB pathway by promoting p65 degradation. *The Journal of Biological Chemistry* **289**, 12578–12592.

Dubey, J. P. and Schares, G. (2011). Neosporosis in animals-The last five years. *Veterinary Parasitology* **180**, 90–108.

Dunn, J. D., Ravindran, S., Kim, S. K. and Boothroyd, J. C. (2008). The *Toxoplasma gondii* dense granule protein GRA7 is phosphorylated upon invasion and forms an unexpected association with the rhoptry proteins ROP2 and ROP4. *Infection and Immunity* **76**, 5853–5861.

El Hajj, H., Demey, E., Poncet, J., Lebrun, M., Wu, B., Galeotti, N., Fourmaux, M. N., Mercereau-Puijalon, O., Vial, H., Labesse, G. and Dubremetz, J. F. (2006). The ROP2 family of *Toxoplasma gondii* rhoptry proteins: proteomic and genomic characterization and molecular modeling. *Proteomics* **6**, 5773–5784.

El Hajj, H., Lebrun, M., Fourmaux, M. N., Vial, H. and Dubremetz, J. F. (2007). Inverted topology of the *Toxoplasma gondii* ROP5 rhoptry protein provides new insights into the association of the ROP2 protein family with the parasitophorous vacuole membrane. *Cellular Microbiology* **9**, 54–64.

Esposito, M., Moores, S., Naguleswaran, A., Muller, J. and Hemphill, A. (2007). Induction of tachyzoite egress from cells infected with the protozoan *Neospora caninum* by nitro- and bromo-thiazolides, a class of broad-spectrum anti-parasitic drugs 9. *International Journal for Parasitology* **37**, 1143–1152.

Etheridge, R. D., Alaganan, A., Tang, K., Lou, H. J., Turk, B. E. and Sibley, L. D. (2014). The *Toxoplasma* pseudokinase ROP5 forms complexes with ROP18 and ROP17 kinases that synergize to control acute virulence in mice. *Cell Host & Microbe* **15**, 537–550.

Fernández-García, A., Risco-Castillo, V., Zaballos, A., Alvarez-García, G. and Ortega-Mora, L. M. (2006). Identification and molecular cloning of the *Neospora caninum SAG4* gene specifically expressed at bradyzoite stage. *Molecular and Biochemical Parasitology* **146**, 89–97.

Gaji, R. Y., Behnke, M. S., Lehmann, M. M., White, M. W. and Carruthers, V. B. (2011). Cell cycle-dependent, intercellular transmission of *Toxoplasma gondii* is accompanied by marked changes in parasite gene expression. *Molecular Microbiology* **79**, 192–204.

Hajagos, B. E., Turetzky, J. M., Peng, E. D., Cheng, S. J., Ryan, C. M., Souda, P., Whitelegge, J. P., Lebrun, M., Dubremetz, J. F. and Bradley, P. J. (2012). Molecular dissection of novel trafficking and processing of the *Toxoplasma gondii* rhoptry metalloprotease toxolysin-1. *Traffic* **13**, 292–304.

Hemphill, A., Vonlaufen, N., Naguleswaran, A., Keller, N., Riesen, M., Guetg, N., Srinivasan, S. and Alaeddine, F. (2004). Tissue culture and explant approaches to studying and visualizing *Neospora caninum* and its interactions with the host cell. *Microscopy and Microanalysis* **10**, 602–620.

Hemphill, A., Debache, K., Monney, T., Schorer, M., Guionaud, C., Alaeddine, F., Mueller, N. and Mueller, J. (2013). Proteins mediating the *Neospora caninum*-host cell interaction as targets for vaccination. *Frontiers in Bioscience (Elite edition)* **5**, 23–36.

Jacot, D. and Soldati-Favre, D. (2012). Does protein phosphorylation govern host cell entry and egress by the Apicomplexa? *International Journal of Medical Microbiology* **302**, 195–202.

Jensen, K. D., Hu, K., Whitmarsh, R. J., Hassan, M. A., Julien, L., Lu, D., Chen, L., Hunter, C. A. and Saeij, J. P. (2013). *Toxoplasma gondii* rhoptry 16 kinase promotes host resistance to oral infection and intestinal inflammation only in the context of the dense granule protein GRA15. *Infection and Immunity* **81**, 2156–2167.

Kemp, L. E., Yamamoto, M. and Soldati-Favre, D. (2013). Subversion of host cellular functions by the apicomplexan parasites. *FEMS Microbiology Reviews* **37**, 607–631.

Kinoshita, E., Kinoshita-Kikuta, E., Takiyama, K. and Koike, T. (2006). Phosphate-binding tag, a new tool to visualize phosphorylated proteins. *Molecular & Cellular Proteomics* **5**, 749–757.

Labruyere, E., Lingnau, M., Mercier, C. and Sibley, L. D. (1999). Differential membrane targeting of the secretory proteins GRA4 and GRA6 within the parasitophorous vacuole formed by *Toxoplasma gondii*. *Molecular and Biochemical Parasitology* **102**, 311–324.

Le Roch, K. G., Johnson, J. R., Florens, L., Zhou, Y., Santrosyan, A., Grainger, M., Yan, S. F., Williamson, K. C., Holder, A. A., Carucci, D. J., Yates, J. R. and Winzeler, E. A. (2004). Global analysis of transcript and protein levels across the *Plasmodium falciparum* life cycle. *Genome Research* **14**, 2308–2318.

Lei, T., Wang, H., Liu, J., Nan, H. and Liu, Q. (2014). ROP18 is a key factor responsible for virulence difference between *Toxoplasma gondii* and *Neospora caninum*. *PLoS ONE* **9**, e99744.

Lescault, P. J., Thompson, A. B., Patil, V., Lirussi, D., Burton, A., Margarit, J., Bond, J. and Matrajt, M. (2010). Genomic data reveal *Toxoplasma gondii* differentiation mutants are also impaired with respect to switching into a novel extracellular tachyzoite state. *PLoS ONE* **12**, e14463.

Lim, D. C., Cooke, B. M., Doerig, C. and Saeij, J. P. (2012). *Toxoplasma* and *Plasmodium* protein kinases: roles in invasion and host cell remodelling. *International Journal for Parasitology* **42**, 21–32.

Llinas, M. and DeRisi, J. L. (2004). Pernicious plans revealed: *Plasmodium falciparum* genome wide expression analysis. *Current Opinion in Microbiology* **7**, 382–387.

Lodoen, M. B., Gerke, C. and Boothroyd, J. C. (2009). A highly sensitive FRET-based approach reveals secretion of the actin-binding protein toxofilin during *Toxoplasma gondii* infection. *Cellular Microbiology* **12**, 55–66.

Lovett, J. L., Howe, D. K. and Sibley, L. D. (2000). Molecular characterization of a thrombospondin-related anonymous protein homologue in *Neospora caninum*. *Molecular and Biochemical Parasitology* **107**, 33–43.

Marugán-Hernández, V., Álvarez-García, G., Tomley, F., Hemphill, A., Regidor-Cerrillo, J. and Ortega-Mora, L. M. (2011). Identification of novel rhoptry proteins in *Neospora caninum* by LC/MS–MS analysis of subcellular fractions. *Journal of Proteomics* **74**, 629–642.

Mercier, C., Adjogble, K. D., Daubener, W. and Delauw, M. F. (2005). Dense granules: are they key organelles to help understand the parasitophorous vacuole of all apicomplexa parasites? *International Journal for Parasitology* **35**, 829–849.

Naguleswaran, A., Cannas, A., Keller, N., Vonlaufen, N., Schares, G., Conraths, F. J., Bjorkman, C. and Hemphill, A. (2001). *Neospora caninum* microneme protein NcMIC3: secretion, subcellular localization, and functional involvement in host cell interaction. *Infection and Immunity* **69**, 6483–6494.

Nakaar, V., Ngô, H. M., Aaronson, E. P., Coppens, I., Stedman, T. T. and Joiner, K. A. (2003). Pleiotropic effect due to targeted depletion of secretory rhoptry protein ROP2 in *Toxoplasma gondii*. *Journal of Cell Science* **116**, 2311–2320.

Pastor-Fernández, I., Arranz-Solís, D., Regidor-Cerrillo, J., Álvarez-García, G., Hemphill, A., García-Culebras, A., Cuevas-Martín, C. and Ortega-Mora, L. M. (2015). A vaccine formulation combining rhoptry proteins NcROP40 and NcROP2 improves pup survival in a pregnant mouse model of neosporosis. *Veterinary Parasitology* **207**, 203–215.

Peixoto, L., Chen, F., Harb, O. S., Davis, P. H., Beiting, D. P., Brownback, C. S., Ouloguem, D. and Roos, D. S. (2010). Integrative genomic approaches highlight a family of parasite-specific kinases that regulate host responses. *Cell Host & Microbe* **8**, 208–218.

Pereira García-Melo, D., Regidor-Cerrillo, J., Collantes-Fernández, E., Aguado-Martínez, A., Del Pozo, I., Minguijon, E., Gómez-Bautista, M., Aduriz, G. and Ortega-Mora, L. M. (2010). Pathogenic characterization in mice of *Neospora caninum* isolates obtained from asymptomatic calves. *Parasitology* **137**, 1057–1068.

Pérez-Zaballos, F. J., Ortega-Mora, L. M., Álvarez-García, G., Collantes-Fernández, E., Navarro-Lozano, V., García-Villada, L. and Costas, E. (2005). Adaptation of *Neospora caninum* isolates to cell-culture changes: an argument in favor of its clonal population structure. *The Journal of Parasitology* **91**, 507–510.

Pittman, K. J., Aliota, M. T. and Knoll, L. J. (2014). Dual transcriptional profiling of mice and *Toxoplasma gondii* during acute and chronic infection. *BMC Genomics* **15**, 806.

Pollo-Oliveira, L., Post, H., Acencio, M. L., Lemke, N., van den Toorn, H., Tragante, V., Heck, A. J., Altelaar, A. F. and Yatsuda, A. P. (2013). Unravelling the *Neospora caninum* secretome through the secreted fraction (ESA) and quantification of the discharged tachyzoite using high-resolution mass spectrometry-based proteomics. *Parasites & Vectors* **6**, 335.

Radke, J. R., Behnke, M. S., Mackey, A. J., Radke, J. B., Roos, D. S. and White, M. W. (2005). The transcriptome of *Toxoplasma gondii*. *BMC Biology* **3**, 26.

Ramaprasad, A., Mourier, T., Naeem, R., Malas, T. B., Moussa, E., Panigrahi, A., Vermont, S. J., Otto, T. D., Wastling, J. and Pain, A. (2015). Comprehensive evaluation of *Toxoplasma gondii* VEG and *Neospora caninum* LIV genomes with tachyzoite stage transcriptome and proteome defines novel transcript features. *PLoS ONE* **10**, e0124473.

Reese, M. L. and Boothroyd, J. C. (2009). A helical membrane-binding domain targets the *Toxoplasma* ROP2 family to the parasitophorous vacuole. *Traffic* **10**, 1458–1470.

Reese, M. L. and Boothroyd, J. C. (2011). A conserved non-canonical motif in the pseudoactive site of the ROP5 pseudokinase domain mediates its effect on *Toxoplasma* virulence. *The Journal of Biological Chemistry* **286**, 29366–29375.

Reese, M. L., Shah, N. and Boothroyd, J. C. (2014). The *Toxoplasma* pseudokinase ROP5 is an allosteric inhibitor of the immunity-related GTPases. *The Journal of Biological Chemistry* **289**, 27849–27858.

Regidor-Cerrillo, J., Gómez-Bautista, M., Pereira-Bueno, J., Adúriz, G., Navarro-Lozano, V., Risco-Castillo, V., Fernández-García, A., Pedraza-Díaz, S. and Ortega-Mora, L. M. (2008). Isolation and genetic characterization of *Neospora caninum* from asymptomatic calves in Spain. *Parasitology* **135**, 1651–1659.

Regidor-Cerrillo, J., Gómez-Bautista, M., Del Pozo, I., Jiménez-Ruiz, E., Aduriz, G. and Ortega-Mora, L. M. (2010). Influence of *Neospora caninum* intra-specific variability in the outcome of infection in a pregnant BALB/c mouse model. *Veterinary Research* **41**, 52.

Regidor-Cerrillo, J., Gómez-Bautista, M., Sodupe, I., Aduriz, G., Álvarez-García, G., Del Pozo, I. and Ortega-Mora, L. M. (2011). *In vitro* invasion efficiency and intracellular proliferation rate comprise virulence-related phenotypic traits of *Neospora caninum*. *Veterinary Research* **42**, 41.

Regidor-Cerrillo, J., Álvarez-García, G., Pastor-Fernández, I., Marugán-Hernández, V., Gómez-Bautista, M. and Ortega-Mora, L. M. (2012). Proteome expression changes among virulent and attenuated *Neospora caninum* isolates. *Journal of Proteomics* **75**, 2306–2318.

Reid, A. J., Vermont, S. J., Cotton, J. A., Harris, D., Hill-Cawthorne, G. A., Konen-Waisman, S., Latham, S. M., Mourier, T., Norton, R., Quail, M. A., Sanders, M., Shanmugam, D., Sohal, A., Wasmuth, J. D., Brunk, B., Grigg, M. E., Howard, J. C., Parkinson, J., Roos, D. S., Trees, A. J., Berriman, M., Pain, A. and Wastling, J. M. (2012). Comparative genomics of the apicomplexan parasites *Toxoplasma gondii* and *Neospora caninum*: Coccidia differing in host range and transmission strategy. *PLoS Pathogens* **8**, e1002567.

Risco-Castillo, V., Fernández-García, A., Zaballos, A., Aguado-Martínez, A., Hemphill, A., Rodríguez-Bertos, A., Álvarez-García, G. and Ortega-Mora, L. M. (2007). Molecular characterisation of BSR4, a novel bradyzoite-specific gene from *Neospora caninum*. *International Journal for Parasitology* **37**, 887–896.

Rojo-Montejo, S., Collantes-Fernández, E., Blanco-Murcia, J., Rodríguez-Bertos, A., Risco-Castillo, V. and Ortega-Mora, L. M. (2009). Experimental infection with a low virulence isolate of *Neospora caninum* at 70 days gestation in cattle did not result in foetopathy. *Veterinary Research* **40**, 49.

Schmittgen, T. D. and Livak, K. J. (2008). Analyzing real-time PCR data by the comparative C(T) method. *Nature Protocols* **3**, 1101–1108.

Schneider, A. G., Abi Abdallah, D. S., Butcher, B. A. and Denkers, E. Y. (2013). *Toxoplasma gondii* triggers phosphorylation and nuclear translocation of dendritic cell STAT1 while simultaneously blocking IFNgamma-induced STAT1 transcriptional activity. *PLoS ONE* **8**, e60215.

Sinai, A. P. and Joiner, K. A. (2001). The *Toxoplasma gondii* protein ROP2 mediates host organelle association with the parasitophorous vacuole membrane. *The Journal of Cell Biology* **154**, 95–108.

Sohn, C. S., Cheng, T. T., Drummond, M. L., Peng, E. D., Vermont, S. J., Xia, D., Cheng, S. J., Wastling, J. M. and Bradley, P. J. (2011). Identification of novel proteins in *Neospora caninum* using an organelle purification and monoclonal antibody approach. *PLoS ONE* **6**, e18383.

Steinfeldt, T., Konen-Waisman, S., Tong, L., Pawlowski, N., Lamkemeyer, T., Sibley, L. D., Hunn, J. P. and Howard, J. C. (2010). Phosphorylation of mouse immunity-related GTPase (IRG) resistance proteins is an evasion strategy for virulent *Toxoplasma gondii*. *PLoS Biology* **8**, e1000576.

Straub, K. W., Cheng, S. J., Sohn, C. S. and Bradley, P. J. (2009). Novel components of the Apicomplexan moving junction reveal conserved and coccidia-restricted elements. *Cellular Microbiology* **11**, 590–603.

Talevich, E. and Kannan, N. (2013). Structural and evolutionary adaptation of rhoptry kinases and pseudokinases, a family of coccidian virulence factors. *BMC Evolutionary Biology* **13**, 117.

Vonlaufen, N., Muller, N., Keller, N., Naguleswaran, A., Bohne, W., McAllister, M. M., Bjorkman, C., Muller, E., Caldelari, R. and Hemphill, A. (2002). Exogenous nitric oxide triggers *Neospora caninum* tachyzoite-to-bradyzoite stage conversion in murine epidermal keratinocyte cell cultures. *International Journal for Parasitology* **32**, 1253–1265.